JOURNAL OF MATERIALS SCIENCE 29 (1994) 4119–4124

The formation of $NaMg_2Al_{15}O_{25}$ in an α-Al_2O_3 matrix and its effect on the mechanical properties of alumina

HAI-DOO KIM, IM-SIK LEE, SUK-WON KANG, JAE-WOONG KO
Ceramic Materials Laboratory, Korea Institute of Machinery and Metals, 66 Sangnam-dong, Changwon, Kyungnam, Republic of Korea

An *in-situ* sintering reaction was designed to produce lath-like β‴-alumina in an α-alumina matrix in order to make alumina ceramics stronger and tougher. The reaction sequence to produce β‴-alumina ($NaMg_2Al_{15}O_{25}$) requires the formation of β-alumina ($NaAl_{11}O_{17}$) and spinel ($MgAl_2O_4$) at around 1100 °C followed by a solid-state reaction of these two phases to give β‴-alumina at elevated temperatures; this reaction is complete at around 1600 °C. The *in-situ* sintering reaction produces near-theoretically dense alumina ceramics in which lath-like β‴-aluminas are homogeneously distributed. The bending strength and fracture toughness increase to 620 MPa and 5 MPa $m^{1/2}$, respectively; these increases are thought to be due to the suppression of grain growth as well as the crack deflection and bridging associated with lath-like β‴-alumina.

1. Introduction

Alumina is one of the most important technical ceramics and has been widely used in various fields because of its attractive properties, such as high wear resistance, high corrosion resistance and high temperature stability. The biggest obstacle for wider applications is probably its low fracture toughness. To overcome this problem, fibres or whiskers have been used to reinforce the matrix. There are, however, many difficulties in this type of toughening. For example, in alumina reinforced by SiC whiskers, there are difficulties in homogeneous mixing, in reaching full densification, in the degradation of SiC whisker in oxidizing atmospheres, and in the danger of the whiskers to health [1–5].

Because the chemical bonding at the interface and the physical nature of the interface govern toughening mechanisms (such as crack deflection, crack branching and debonding behaviour [6]), the use of fibres or whiskers in ceramic-matrix composites gives rise to considerable interfacial problems, which sometimes necessitates surface coating of the fibres or whiskers; one possible solution is an *in situ* sintering reaction to form the reinforcement in the matrix.

In alumina technology, MgO is the most widely used sintering additive. Na_2O is the major impurity and it is difficult to avoid [7–9]. The widely used Bayer-processed alumina powders contain 0.05 to 0.5 wt % Na_2O, which gives rise to a considerable amount of the second phase (β-alumina) after sintering. The formation of β-alumina ($NaAl_{11}O_{17}$) in the α-alumina matrix is undesirable because of its thermal instability [10]. One of the thermally stable β-type aluminas is $NaMg_2Al_{15}O_{25}$; it is called β‴-alumina [11]. β‴-alumina is a very useful phase in alumina technology because the formation of β‴-alumina in the α-alumina matrix can scavenge the Na impurity, which can lead to the possibility of the incorporation of this undesirable impurity in the useful form [12]. In this study, β‴-alumina was introduced in the α-alumina matrix by an *in situ* sintering reaction, and its influence on the mechanical properties was investigated.

2. Experimental procedure

2.1. Sample preparation

In order to form various amounts of the $NaMg_2Al_{15}O_{25}$ phase in the α-alumina matrix, the composition was chosen as $(100 - 5x)Al_2O_3 + x(Na_2O + 4MgO)$, where x was 0, 0.5, 1.0, 1.5 and 3.0 mol. Mg-acetate ($(CH_3COO)_2 Mg \cdot 4H_2O$, Merck Art. 5819) and Na_2CO_3 (Merck Art. 6392) were dissolved in distilled water in the ratio Na : Mg = 1 : 2 and the appropriate amounts of Al_2O_3 (AKP-30, Sumitomo, Japan) were added to this solution. The equilibrium composition after sintering, with respect to x, was calculated by rational analysis and it is tabulated in Table I.

The wet mixture was dried under an infrared (i.r.) lamp while stirring, and then calcined at 850 °C in air. After calcination, the powder mixture was gently ground and the pressed tablets were sintered at 1600 °C for various times. The calcined powder mixture was also hot-pressed at 1550 °C or 1600 °C for 30 min under a pressure of 30 MPa, in vacuum, or in an Ar atmosphere using a graphite mould with an inside diameter of 30 mm.

0022–2461

TABLE I A prediction of the phases formed, on the basis of a rational-analysis

	Phases (wt %)	
x	α-Al_2O_3	β'''-alumina ($NaMg_2Al_{15}O_{25}$)
0	100	0
0.5	91.3	8.7
1.0	82.4	17.6
1.5	73.2	26.8
3.0	43.4	56.6

2.2. Measurements

The density was determined by the Archimedes principle. The microstructures were investigated using optical microscopy and scanning electron microscopy (SEM) after polishing and thermal etching. For the bending-strength measurements, the sintered tablets were cut into a $3 \times 4 \times 25\ mm^3$ bar, then ground and finally polished with a 1 μm diamond paste. The three-point bending strength was determined using a universal testing machine with a span of 18 mm at a crosshead speed of $0.5\ mm\ min^{-1}$ and at least five measurements were made for each condition. The fracture toughness was measured by the Vickers indentation method [13] using a 10 kg load, taking at least 20 measurements for each sample.

To understand the reaction sequence between Al_2O_3 and small amounts of Na_2O and MgO, a composition with $x = 1.0$ was chosen. The pressed tablets were sintered at 1500 °C for 0.24 h, 1600 °C for 0.24 h, and 1600 °C for 24 h. An X-ray powder diffractometer with a CuK_α target was used at 30 kV and 30 mA. To calculate the relative fractions of each phase the following peaks were used: (0 1 2) for Al_2O_3, (0 0 4) for $NaAl_{11}O_{17}$, (1 1 1) for $MgAl_2O_4$ and (0 0 4) for $NaMg_2Al_{15}O_{25}$.

3. Results

3.1. Reaction sequence in the formation of $NaMg_2Al_{15}O_{25}$

The schematic reaction sequence in the system, 95 mol Al_2O_3 + 1 mol Na_2O + 4 mol MgO, is shown in Fig. 1. At 1500 °C for 0.24 h sintering, Al_2O_3 is the major phase and $MgAl_2O_4$ and $NaAl_{11}O_{17}$ appear as secondary phases. The amounts of $MgAl_2O_4$ and $NaAl_{11}O_{17}$ formed were reduced at 1600 °C for 0.24 h sintering and $NaMg_2Al_{15}O_{25}$ started to appear. At 1600 °C for 24 h sintering, the only secondary phase to appear was $NaMg_2Al_{15}O_{25}$. This result suggests that the $NaMg_2Al_{15}O_{25}$ phase forms by consuming the $MgAl_2O_4$ and $NaAl_{11}O_{17}$ phases. The composition of β'''-alumina is $NaMg_2Al_{15}O_{25}$, which is the summation of $NaAl_{11}O_{17}$ and 2 mol of $MgAl_2O_4$. Therefore, it is presumed that 1 mol of $NaAl_{11}O_{17}$ and 2 mol of $MgAl_2O_4$ react to form β'''-alumina. $NaAl_{11}O_{17}$ forms at around 1000 °C [14] and spinel forms at around 900–1250 °C [15]. Therefore, $NaAl_{11}O_{17}$ and $MgAl_2O_4$ form at around 1000–1250 °C and, with increasing temperatures, both react with each other to give $NaMg_2Al_{15}O_{25}$ and this reaction is terminated at 1600 °C.

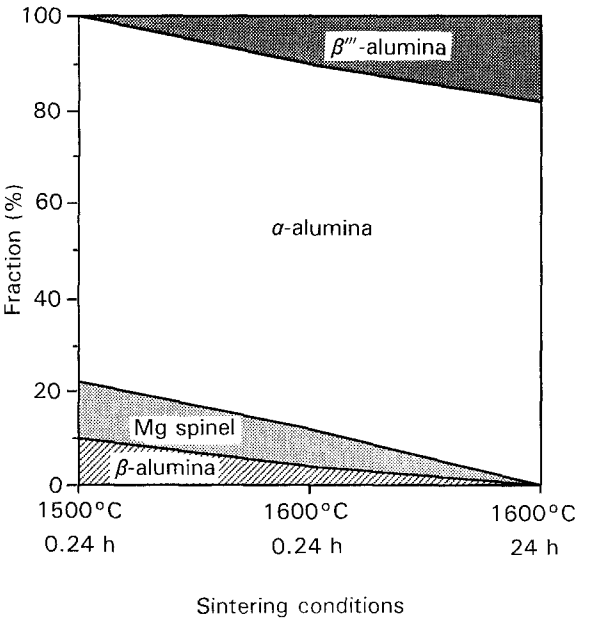

Figure 1 Schematic reaction sequence in the system $95Al_2O_3 + Na_2O + 4MgO$ for different sintering conditions, measured by X-ray diffraction.

3.2. Mechanical properties

The change in density with different amounts of β'''-alumina is shown in Fig. 2. A decrease in the density as increasing amounts of β'''-alumina are formed is understandable because the theoretical density of β'''-alumina is lower than that of α-alumina, although the exact theoretical density of β'''-alumina is not known. According to Bettman and Turner [11], β'''-alumina consists of a hexagonal structure with $a_0 = 0.562$ nm and $c_0 = 3.18$ nm. If the chemical formula and lattice parameters used are correct, the theoretical density of β'''-alumina is calculated to be $3161\ kg\ m^{-3}$, although the powder density for single-phase β'''-alumina was measured in our laboratory as $3500\ kg\ m^{-3}$. Fig. 2 also suggests that hot pressing is very effective in increasing the density even in the region of large amounts of β'''-alumina.

Fig. 3 shows the large increase in the bending strength when β'''-alumina is formed in an α-alumina

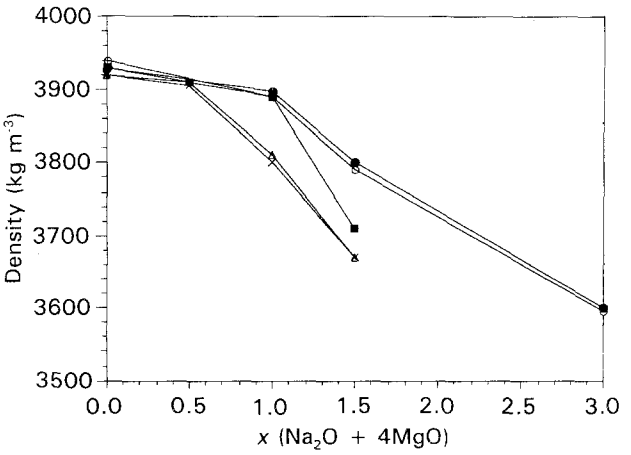

Figure 2 Change in density with different amounts of β'''-alumina: (○) hot pressed (1550 °C, 30 min, 30 MPa, in Ar); (●) hot pressed (1600 °C, 30 min, 60 MPa, in Ar); (×) 1600 °C, 1 h; (△) 1600 °C, 3 h; and (■) 1600 °C, 10 h.

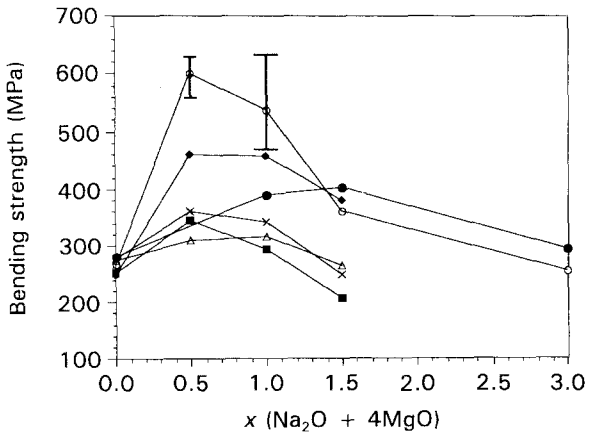

Figure 3 Change in bending strength with different amounts of β‴-alumina: (○) hot pressed (1550 °C, 30 min, 30 MPa, in Ar); (◆) hot pressed (1600 °C, 30 min, 30 MPa, in Ar); (●) hot pressed (1600 °C, 30 min, 60 MPa, in Ar); (×) 1600 °C, 1 h, (△) 1600 °C, 3 h; and (■) 1600 °C, 10 h.

matrix. When x is 0.5, the bending strength is about 600 MPa which is more than twice that of alumina containing no β‴-alumina. The maximum bending strength is when x is between 0.5 and 1.0; beyond this range the bending strength decreases. The pressureless sintering did not result in a large increase in the bending strength.

Fig. 4 shows the microstructural development with increases in the amount of β‴-alumina formed. When x is 0.5 or 1.0, a considerable amount of lath-like β‴-alumina formed in the α-alumina matrix, and all the β‴-alumina remains as discrete phase in the matrix, while the β‴-alumina grains touch each other when $x = 1.5$.

The formation of β‴-alumina in the α-alumina matrix has a very pronounced impact on the grain-growth inhibition of α-alumina matrix. Fig. 5 shows quantitative data for the specimen sintered at 1600 °C for a prolonged time. As expected, the grain size of the α-alumina matrix increases as the sintering time increases. As the x-value increases, that is, as the amount of β‴-alumina formed in the α-alumina matrix increases, the grain size of the α-alumina decreases and this is possibly one of the reasons why the α-alumina/β‴-alumina shows higher bending strengths.

In order to see why there is an optimal amount of β‴-alumina in the α-alumina matrix, more detailed microstructures are shown in Fig. 6. When x is 0.5 or 1.0, the β‴-alumina laths are discrete in the α-alumina matrix, while, for $x = 1.5$, they touch to form a network in which lots of pores are located at grain boundaries of the α-alumina matrix. It seems that, once the β‴-alumina laths grow to form a network, it is very hard for the grains inside the network to sinter, and the pores remaining are responsible for the lower strength.

The fracture toughness increased when β‴-alumina formed in the α-alumina matrix (Fig. 7). Hot-pressed specimens showed higher values than pressureless-sintered specimens, and the highest fracture toughness was obtained when x equalled 1.0. The mode of crack propagation after indentation is shown in Fig. 8. Both

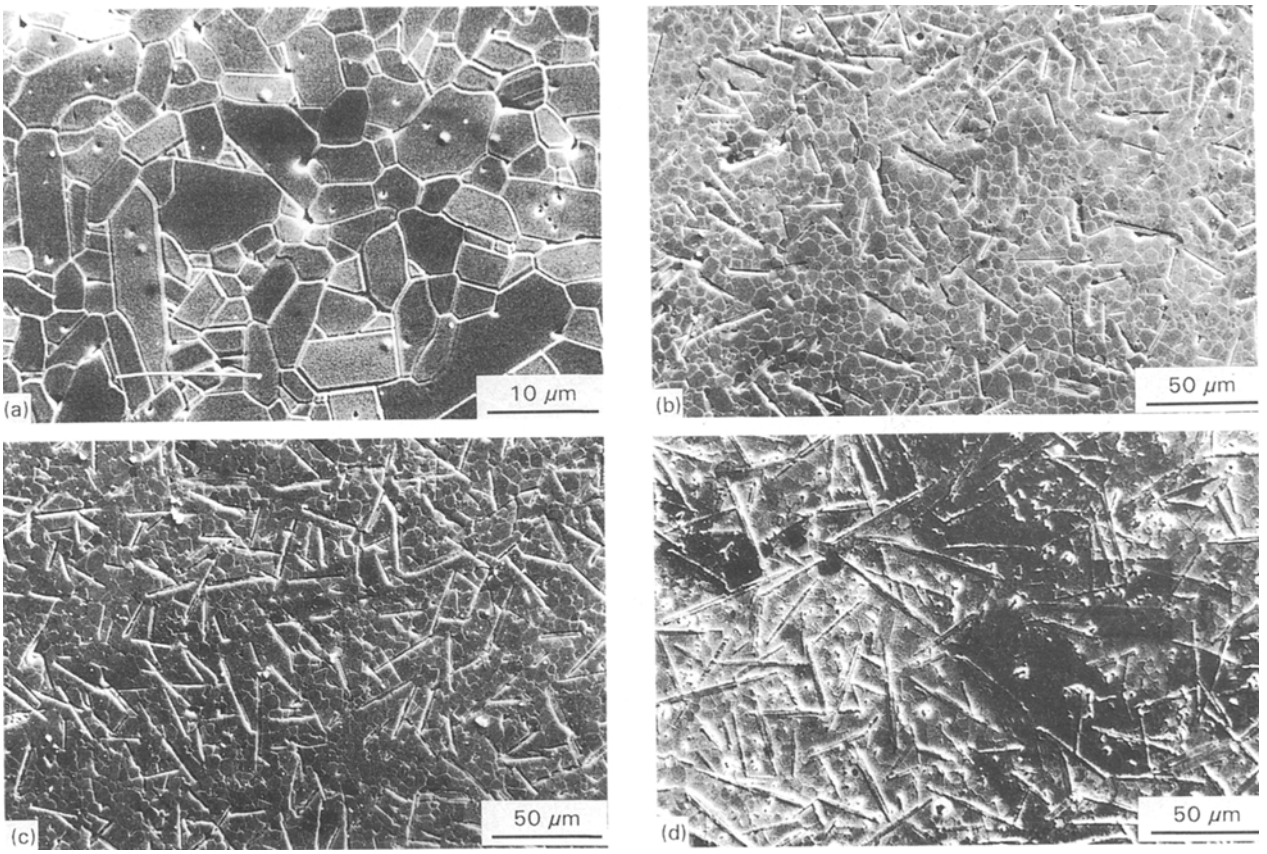

Figure 4 Microstructures of the specimens in the system $(100 - 5x)\,Al_2O_3 + x(Na_2O + 4MgO)$ sintered at 1600 °C for 10 h, where (a) $x = 0$, (b) $x = 0.5$, (c) $x = 1.0$, and (d) $x = 1.5$.

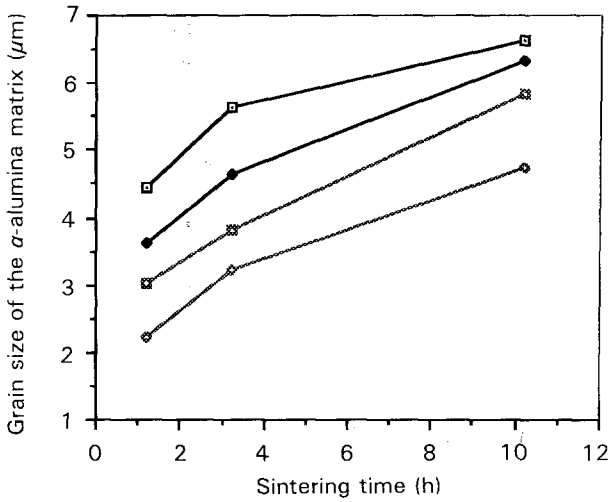

Figure 5 Change in the grain size of the α-alumina matrix with different sintering times (the β‴-alumina is disregarded): (⊡) $x = 0$, (◆) $x = 0.5$, (□) $x = 1.0$ and (◇) $x = 1.5$ (the sintering temperature was 1600 °C).

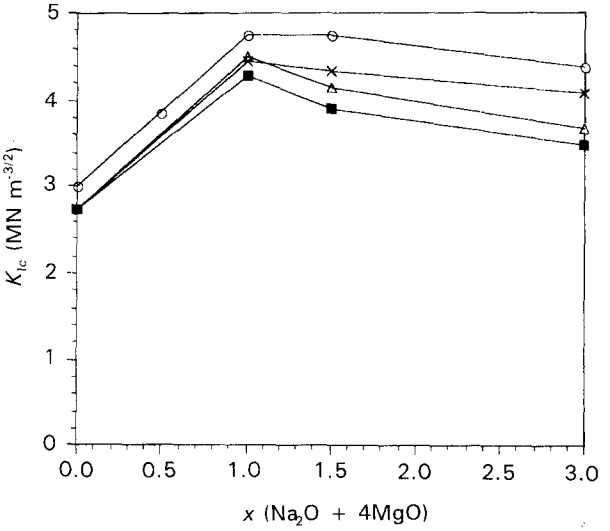

Figure 7 The change in the fracture toughness of the specimens with different amounts of β‴-alumina: (○) hot pressed (1550 °C, 30 min, 30 MPa, in Ar); (×) 1600 °C, 1 h; (△) 1600 °C, 3 h; (■) 1600 °C, 10 h.

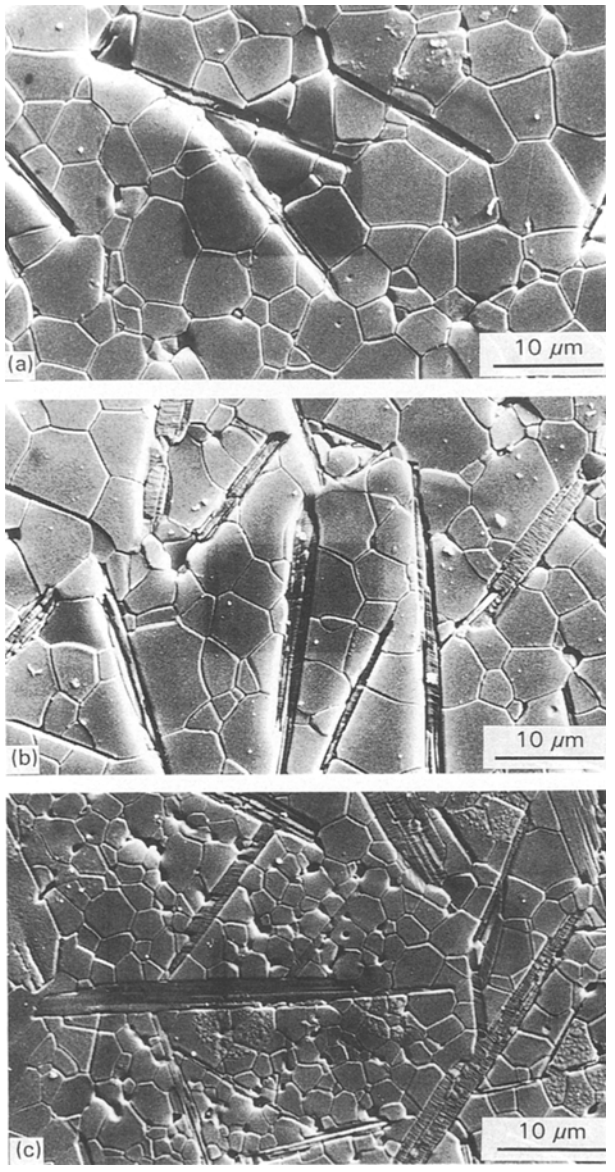

Figure 6 Microstructures of the specimen sintered at 1600 °C for 10 h for the following x-values: (a) $x = 0.5$, (b) $x = 1.0$, and (c) $x = 1.5$.

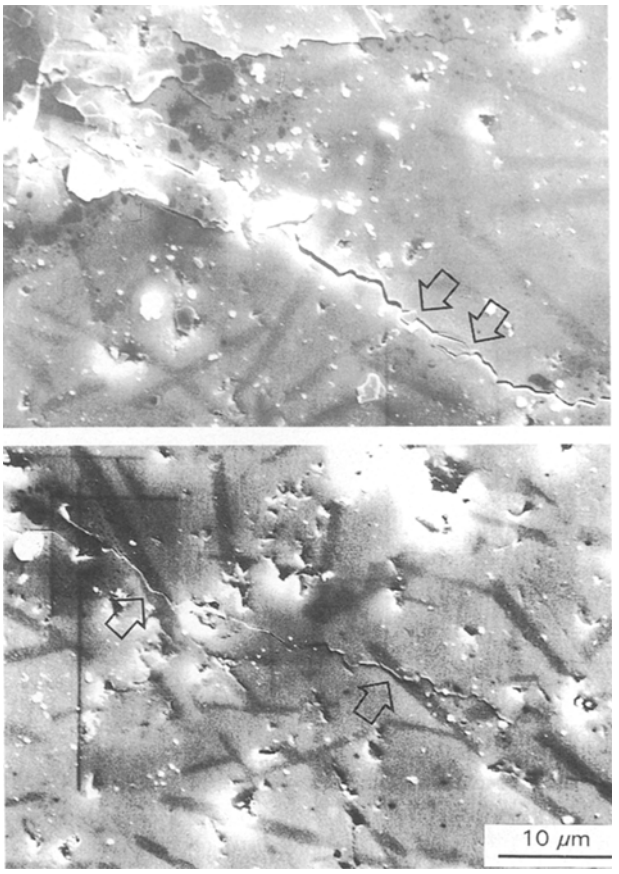

Figure 8 Crack propagation mode of the specimen in the system $92.5Al_2O_3 + 1.5(Na_2O + 4MgO)$ after hot-pressing in a vacuum at 1550 °C for 30 min.

crack deflection and crack bridging are observed, and they seem to be the major mechanisms contributing to the toughening of the matrix.

4. Discussion

The major difficulty in understanding the sintering behaviour of this system is that solid-state reactions as

well as sintering phenomena occur simultaneously. In this experiment, near-theoretical density was achieved, although the lath-like second phase was formed during a solid-state reaction. Fig. 4 shows the homogeneous distribution of lath-like β‴-aluminas in a well-sintered α-alumina matrix. In order to see the sintering behaviour of alumina with and without β‴-alumina formation, the shrinkage behaviour was investigated with increasing temperature (Fig. 9). At each temperature less shrinkage occurred when secondary phases formed by a solid-state reaction and, at high temperatures such as 1600 °C, the difference in the shrinkage was less pronounced. The results above may suggest that the secondary phases hinder grain growth and densification of the α-alumina matrix at moderate temperatures. This may also result in the pores remaining attached at the grain boundaries, which is a favourable situation for matrix sintering at higher temperatures. Also, as shown in Fig. 6, sintering will occur until the formation of a network by lath-like β‴-alumina. Therefore, if the formation of a network by the lath-like phase can be avoided during reaction sintering, near-theoretical density can be achieved.

The bending strength was increased by the formation of β‴-alumina in the α-alumina matrix. From the investigation of the microstructure, the most pronounced effect of β‴-alumina formation in the α-alumina matrix is grain-growth inhibition of α-alumina (Figs 4 and 6). That means that the introduction of β‴-alumina into α-alumina matrix during sintering can hinder the grain growth of the α-alumina matrix (Fig. 5). The β‴-alumina formed will be able to act as a phase boundary and thus prevent the material transport of the components, so the sintering of the α-alumina matrix will be retarded. Besides, lath-like β‴-alumina can inhibit the grain-boundary movement, which is a prerequisite for grain growth. Even very small amounts of MgO can act as a grain-growth inhibitor.

The increase in toughness is thought to be due to the crack deflection and crack bridging. The crack

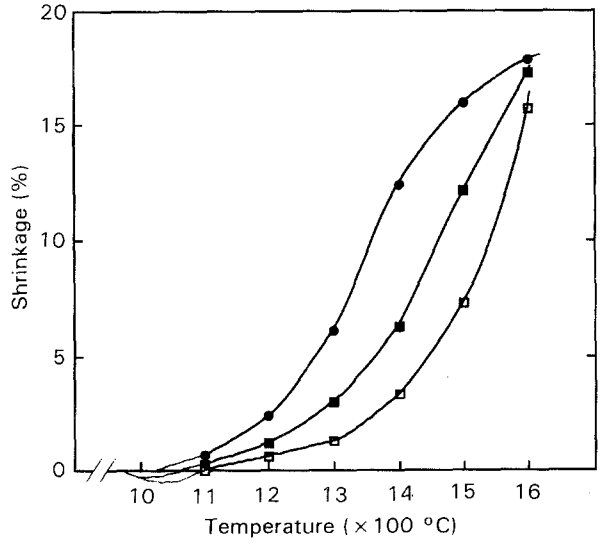

Figure 9 Shrinkage behaviour of the specimens during sintering: (●) Al_2O_3, (■) $95Al_2O_3$ + 1.0 (Na_2O + 4MgO), and (□) $92.5Al_2O_3$ + 1.5 (Na_2O + 4MgO).

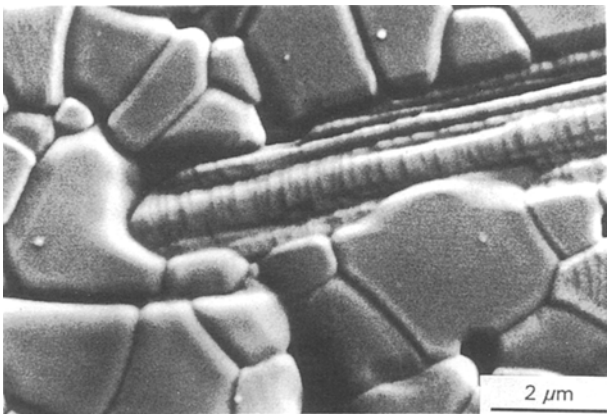

Figure 10 Morphology of β‴-alumina showing lamellar structure.

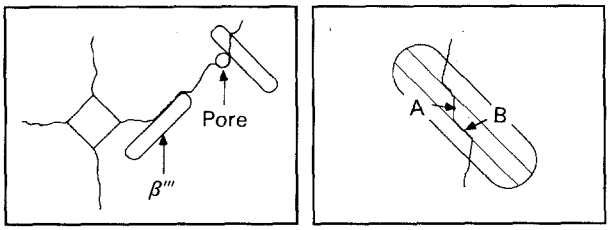

Figure 11 Schematic diagram of crack propagation.

bridging seems to be the major contributor to the increase in the toughness. Lawn *et al.* [16–17] showed that the flaw-insensitive concept with the alumina in which Al_2TiO_5 grains are homogeneously, distributed in an α-alumina matrix through reaction sintering. In an α-Al_2O_3/Al_2TiO_5 composite, the bending strength and fracture toughness were not dependent on the flaw size. Lawn *et al.* insisted that the major mechanism is the crack-bridging process due to the Al_2TiO_5 particles. This situation can be presumed in α-alumina/β‴-alumina composites. When the morphology of β‴-alumina laths are seen at high magnifications, a lamellar structure is visible (Fig. 10). Therefore, when a crack tip meets a β‴-alumina lath, the crack tip does not propagate straight through the β‴-alumina lath but can deflect depending on the incident angle. Fig. 11 shows the proposed mechanism of crack propagation, in which translamellar (A) and interlamellar (B) fracture can occur.

5. Conclusion

In situ reaction sintering forming β‴-alumina in an α-alumina matrix results in higher bending strengths and fracture toughnesses than are achieved without β‴-alumina. The higher bending strength is thought to be due to a grain-growth inhibiting effect and the higher fracture toughness is thought to be due to crack-deflection and crack-bridging mechanisms. In the reaction sequence in the formation of β‴-alumina, $NaAl_{11}O_{17}$ (β-alumina) and $MgAl_2O_4$ (Mg spinel) are formed at around 1100 °C followed by a solid-state reaction of these two phases to give β‴-alumina. This reaction is complete at around 1600 °C.

Acknowledgement

The authors thank the Ministry of Science and Technology, Korea for providing the funding for this program.

References

1. J. HOMENY, W. L. VAUGHN and M. K. FERBER, *Amer. Ceram. Soc. Bull.* **67** (1987) 333.
2. G. C. WEL and P. F. BECHER, *ibid.* **64** (1985) 298.
3. T. N. TIEGS and P. F. BECHER, *ibid.* **66** (1987) 339.
4. M. D. SACKS, H. W. LEE and O. E. ROJAS, *J. Amer. Ceram. Soc.* **71** (1988) 370.
5. T. N. TIEGS and P. F. BECHER, in "Tailoring multiphase and composite ceramics" Vol. 20. (Plenum Press, New York, 1986) p. 639.
6. K. B. ALEXANDER, P. ANGELINI, and P. F. BECHER, in "Ceramic transactions" Vol. 19. (The American Ceramic Society, Westerville, OH, 1991) p. 245.
7. P. REIJNEN and H. D. KIM, Ceramic Forum International/Berichte der Deutschen Keramischen Gesellschaft **63** (1986) 272.
8. *Idem.*, in Proceedings of the 8th Yugoslav–German Meeting on Materials Science and Development, May 1987, Ljobljana, Yugoslavia (1987) p. 91.
9. H. D. KIM and P. REIJNEN, in Proceedings of the 10th Korean Symposium on Science and Technology, July 1987, Seoul, Korea (1987) p. 179.
10. A. K. RAY and E. C. SUBBARAO, *Mater. Res. Bull.* **10** (1975) 583.
11. M. BETTMAN and L. L. TERNER, *Inorg. Chem.* **10** (1971) 1442.
12. P. REIJNEN, *Mater. Sci. Res.* **13** (1979) 355.
13. B. R. LAWN and E. R. FULLER, *J. Mater. Sci.* **10** (1975) 2016.
14. C. M. P. M. SARIS and H. VERWEIJ, *Solid State Ionics* **16** (1985) 185.
15. S. J. KISS, E. KOSTIC and S. B. SKOVIC, *Sci. Ceram.* **12** (1984) 195.
16. S. J. BENNISON, N. P. PADTURE, J. L. RUNYAN and B. R. LAWN, *Philos. Mag. Lett.* **64** (1991) 191.
17. N. P. PADTURE, S. J. BENNISON and H. M. CHAN, *J. Am. Ceram. Soc.* **76** (1993) 2312.

Received 3 September 1992
and accepted 3 June 1993